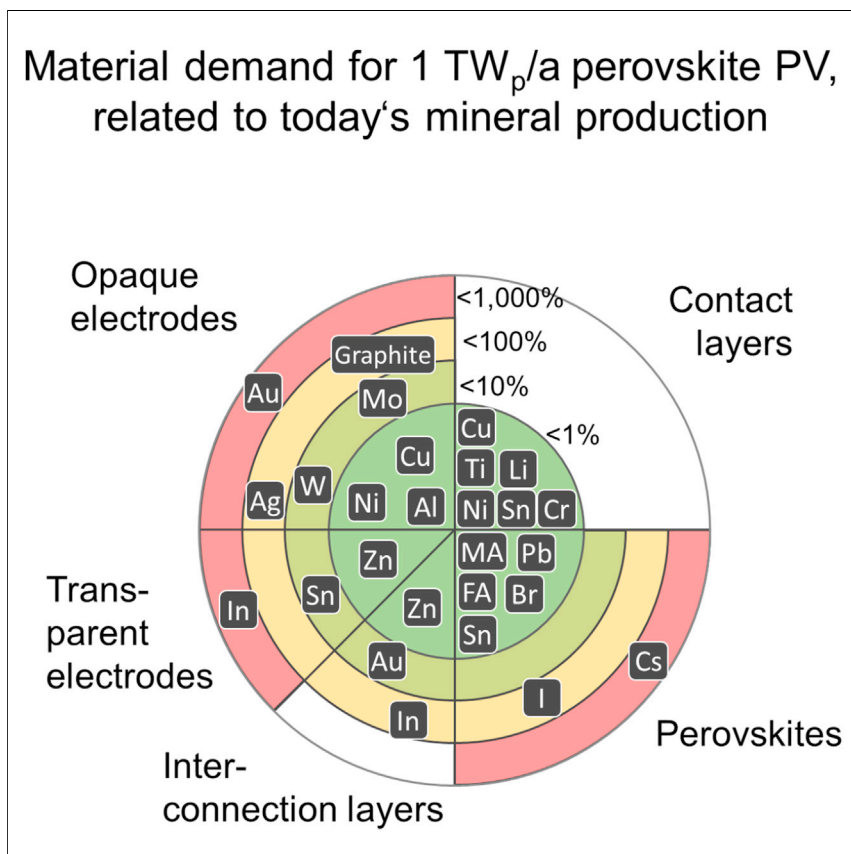


Article

# The resource demands of multi-terawatt-scale perovskite tandem photovoltaics



Lukas Wagner, Jiajia Suo, Bowen Yang, ..., Robert Pietzcker, Andrea Gassmann, Jan Christoph Goldschmidt  
lukas.wagner@physik.uni-marburg.de

**Highlights**

Multi-TW-scale production of perovskite PV will consume large amounts of materials

Most materials for functional layers are abundantly available

Materials In, Au, and Cs are associated with high supply criticality

Industrial production of organic charge-transport materials must be targeted

The resource demand of multi-terawatt scale production of perovskite photovoltaics was assessed. Resource criticalities require replacement of materials frequently used in research, such as indium and gold used in electrodes and cesium used in perovskite photoabsorbers. For most organic hole-transport materials, scalable production needs to be urgently demonstrated. Overall, multi-terawatt-scale production of perovskite PV is feasible.

Wagner et al., Joule 8, 1142–1160  
April 17, 2024 © 2024 The Author(s). Published by Elsevier Inc.  
<https://doi.org/10.1016/j.joule.2024.01.024>



Article

# The resource demands of multi-terawatt-scale perovskite tandem photovoltaics

Lukas Wagner,<sup>1,7,\*</sup> Jiajia Suo,<sup>2</sup> Bowen Yang,<sup>2</sup> Dmitry Bogachuk,<sup>3,6</sup> Estelle Gervais,<sup>3</sup> Robert Pietzcker,<sup>4</sup> Andrea Gassmann,<sup>5</sup> and Jan Christoph Goldschmidt<sup>1</sup>

## SUMMARY

Photovoltaics (PV) and wind are the most important energy-conversion technologies for cost-efficient climate change mitigation. To reach international climate goals, the annual PV module production must be expanded to multi-terawatt (TW) scale. Economic and resource restraints demand the implementation of cost-efficient multi-junction technologies, for which perovskite-based tandem technologies are highly promising. In this work, the resource demand of the emerging perovskite PV technology is investigated, considering two factors of supply criticality, namely, mining capacity for minerals and the production capacity for synthetic materials. Overall, the expansion of perovskite PV to a multi-TW scale may not be limited by material supply if certain materials, especially indium, can be replaced. Moreover, organic charge-transport materials face currently unresolved scalability challenges. This study demonstrates that, besides the improvement of efficiency and stability, perovskite PV research and development also need to be guided by sustainable materials choices and design-for-recycling considerations.

## INTRODUCTION

To limit planetary warming, cross-sectoral rapid transitions are essential. In the energy sector, photovoltaics (PV) is the most important energy conversion technology considering also cost efficiency.<sup>1,2</sup> Therefore, a continued drastic expansion of PV module production is needed, which implies that the PV industry is set to enter multi-terawatt (TW) module production in the coming years.<sup>3</sup> In a recent study, we assessed the resource demand of such multi-TW PV production scenarios, applying technological learning models to the current, wafer-based silicon PV market. We found that although the demand for silver and glass, as well as energy and associated greenhouse gas emissions, are critical, there are no fundamental resource restraints if supply does not decrease and technological learning can be maintained at a high level.<sup>4</sup> Yet, in the study we already outlined that the projected necessary performance increase of PV will surpass the fundamental efficiency limit of silicon PV,<sup>5</sup> which mandates the introduction of novel PV technologies. The candidates with the highest technology readiness level to overcome the single-junction efficiency limit are tandem or multi-junction architectures where multiple solar cells are stacked on top of each other to enable selective harvesting of distinct fractions of the solar spectrum.<sup>6</sup> Because simultaneously, energy demand for solar cell productions needs to be reduced considerably, metal halide perovskites have emerged as highly promising semiconductors for both perovskite/silicon tandem (PST) in the short-term and all-perovskite tandem (APT) devices in the long-term due to their favorable semiconductor properties and processability at ambient conditions with

## CONTEXT & SCALE

Cost-efficient climate change mitigation mandates the rapid expansion of photovoltaic (PV) module production to multi-terawatt (TW) scale. Such an expansion requires enormous material and energy streams. Perovskite-based tandem solar cells are widely regarded as helpful in solving these issues as they promise higher efficiencies and overall lower materials demands. This work presents a comprehensive quantitative assessment of the material demands and potential supply criticalities for multi-TW perovskite PV.

Severe supply risks are identified for a range of materials that are widely used in high-performing perovskite PV devices: cesium used in perovskite alloys, indium employed in transparent electrodes, gold used in back electrodes, as well as most organic contact layers. These results can be regarded as a wake-up call for the perovskite PV research community to reassess current research directions and align them with long-term sustainability considerations. As promising alternatives exist, the expansion of perovskite PV to a multi-TW scale may not be limited by material supply.



industrially established coating techniques. Today, the efficiency of PST already surpasses the performance limit of silicon devices.<sup>7–10</sup>

This high potential has led to tremendous research activities on perovskite solar cells (PSCs). The vast majority of scientific publications have focused on increasing the power conversion efficiency and stability of laboratory-scale devices (Figure S1). On par with increasing industry activities, there is also a growing trend toward advancing scalability. Fewer studies have been published on questions of sustainability, with a focus on the toxicity of lead or life-cycle assessments.<sup>11–13</sup> Few papers have investigated the supply criticality of individual materials used in perovskite PV stacks, such as lead and iodine,<sup>14–16</sup> bromine,<sup>16</sup> cesium,<sup>16</sup> and indium.<sup>15</sup> However, a study assessing a comprehensive inventory of materials relevant for perovskite PV is still pending. Although it has often been claimed a priori that PSCs are made from abundant materials,<sup>17–20</sup> the fundamental question whether the materials and processes necessary for all individual layers in PSC stacks and APT solar cell stacks will be available for multi-TW-scale PV production has not been addressed yet.

In this work, we investigate the hypothesis of resource abundance quantitatively, assess the material demand for a multi-TW-scale perovskite PV production, identify potential supply risks for each material, and derive guidelines for further device optimization and material research. The study is based on a model for future multi-TW perovskite PV production that is coupled to an inventory of the most relevant materials used for PSC production. We find that most materials currently used in perovskite research are likely not linked to a supply risk, although replacements for some commonly used materials need to be found. Two factors of supply criticality are assessed, namely primary production of minerals as well as the production capacity for synthetic materials. This approach exceeds the established demand-to-production assessment, highlighting that scaling production from research to industrial levels should also be part of resource availability analyses. In agreement with previous studies,<sup>15</sup> we identify an urgent need to replace the commonly used metal indium which is employed in transparent electrodes. Moreover, contrasting to previous publications,<sup>16</sup> cesium used in many perovskite alloys is associated with high supply risks. Production of halides and the most promising organic solvents to coat perovskite layers require moderate scale-up. With the exception of PEDOT:PSS, the currently used organic hole-transport materials (HTMs) will only be expedient for multi-TW-scale perovskite PV production if the current material synthesis can be scaled by a factor of more than 10,000 times.

## RESULTS

### Perovskite PV industry growth scenario

We base our assessment on a scenario for the growth of global PV capacity in compliance with limiting planetary warming to below 1.5°C, calculated within the REMIND model.<sup>21</sup> Our scenario projects a continuous growth of the installed PV capacity until the end of the century, starting with historical data of global installed PV capacity of approximately 190 GW<sub>p</sub> in 2021.<sup>22</sup> In line with PV industry roadmaps,<sup>6</sup> the scenario yields a installed capacity of 704 GW<sub>p</sub>/a in 2030 (Figure 1A). The 1 TW<sub>p</sub>/a milestone is surpassed in 2046, and a production of 4 TW<sub>p</sub>/a is reached in 2100. This corresponds to a cumulative installed PV capacity of 21.7 TW<sub>p</sub> by 2050, and 84.5 TW<sub>p</sub> by 2100. These projections fall below historical compound annual growth rates (CAGRs)<sup>22</sup> and most other 100% renewable energy scenarios assign similar or higher PV capacity expansion rates by 2050.<sup>1,4</sup> Hence, the estimated material demand should be considered as conservative assessments.

<sup>1</sup>Physics of Solar Energy Conversion Group, Department of Physics, Philipps-University Marburg, Renthof 7, 35037 Marburg, Germany

<sup>2</sup>Department of Chemistry, Ångström Laboratory, Uppsala University, Box 523, 75120 Uppsala, Sweden

<sup>3</sup>Fraunhofer Institute for Solar Energy Systems ISE, Heidenhofstr. 2, 79110 Freiburg, Germany

<sup>4</sup>Potsdam Institute for Climate Impact Research, P.O. Box 60 12 03, 14412 Potsdam, Germany

<sup>5</sup>Fraunhofer Research Institution for Materials Recycling and Resource Strategies IWKS, Brentanostr. 2a, 63755 Alzenau, Germany

<sup>6</sup>Present address: Solarlab Aiko Europe GmbH, Berliner Allee 29, 79110 Freiburg, Germany

<sup>7</sup>Lead contact

\*Correspondence: [lukas.wagner@physik.uni-marburg.de](mailto:lukas.wagner@physik.uni-marburg.de)  
<https://doi.org/10.1016/j.joule.2024.01.024>

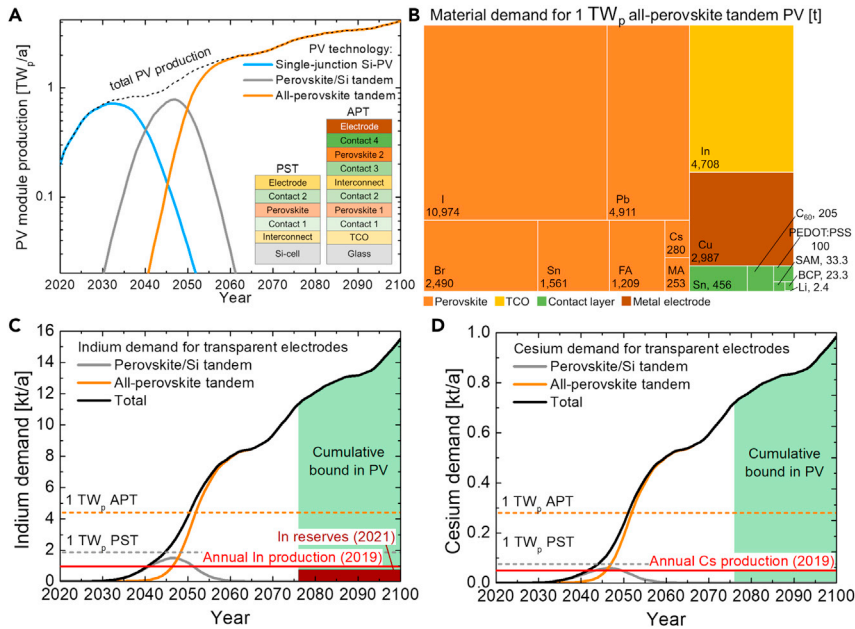


**Figure 1. Growth scenarios and material demand for multi-terawatt scale perovskite photovoltaics**

(A) Modeled PV module production compatible with an energy infrastructure to reach the 1.5°C climate goal. The scenario considers a technology shift from single-junction silicon PV to perovskite-silicon tandem (PST) peaking in 2047 to all-perovskite tandem (APT) PV. The insets illustrate the layer sequence of typical PST and APT devices (TCO, transparent conductive oxide). (B) Material demand in metric tons to produce 1 TW<sub>p</sub> of a representative APT device configuration<sup>23</sup> (see Tables S1 and S2 and supplemental information section “materials and layer inventory”). The considered layer stack is IO:H/SAM/FA<sub>0.8</sub>Cs<sub>0.2</sub>Pb(I<sub>0.62</sub>Br<sub>0.38</sub>)<sub>3</sub>/LiF/C<sub>60</sub>/SnO<sub>2</sub>/ITO/PEDOT:PSS/FA<sub>0.7</sub>MA<sub>0.3</sub>Pb<sub>0.5</sub>Sn<sub>0.5</sub>I<sub>3</sub>/C<sub>60</sub>/BCP/Cu (SAM, self-assembled monolayer). The total material demand of the exemplary solar cell layer stack for 1 TW<sub>p</sub> is 30,194 t. (C and D) Annual material demand resulting from the PV growth model for (C) indium used in transparent electrodes and (D) cesium used in perovskites for PST (gray) and APT (orange) devices. Dashed lines indicate the demand for 1 TW<sub>p</sub>. The solid red line represents the annual In or Cs production in 2019. The green areas under the curve represent the largest amount of materials bound in the PV infrastructure in the considered scenarios, assuming module lifetimes of 25 years. For comparison, the area of the dark red box illustrates currently known In reserves of 18.8 kt.<sup>24</sup> Cs reserves are estimated to be 200 kt.<sup>25</sup>

With a market share of 95%, the current global PV module production mainly consists of wafer-based silicon PV technology,<sup>22</sup> which experienced an increase in power conversion efficiency of 7.9% relative for each doubling of the cumulative production capacity.<sup>6</sup> To maintain such learning rates, the International Technology Roadmap for Photovoltaic 2022 (ITRPV) forecasts that the first tandem devices will enter the mass market between 2024 and 2026, gaining a market share of approximately 5% by 2032.<sup>6</sup> This will likely be realized by PST solar cell stacks which possess the highest technological readiness levels (TRLs) of 7–8 with the company, Oxford PV, planning to start commercial production within 2023.<sup>26</sup> It is reasonable to assume that, once perovskite PV technology is established with the industrial production of PST, the full economic prospects will be harnessed by replacing wafer-based PST with thin-film APT solar cell stacks, which are currently at a TRL of 3. Consequently, we model the market entry of both PST and APT PV technologies, assuming that a 50% market share will be reached in 2040 for PST PV and in 2050 for APTs (Figure 1A). Due to the high uncertainty regarding potential market entries, implementations of triple- and higher-order junction perovskite PV are not assessed here.

Moreover, the focus on tandems does not exclude a market potential for single-junction perovskite PV or other tandem configurations than those assessed in this paper (e.g., triple-junction solar cell stacks or four-terminal architectures fabricated on separate substrates). For any of these technologies, the general material inventory is covered in our analysis, meaning that the PSC stacks will be manufactured from the same types of materials, whereas the exact material demands will scale with the number of junctions and depend on the chosen configurations. Our estimates should not be understood as a market outlook but rather a plausible assessment of the resource requirements if the global demand for PV modules would be fulfilled with perovskite tandem devices.

### Material demand for multi-TW-scale perovskite PV

We have previously highlighted the criticality in supply of the resource of glass used as PV module substrate and potential back-sheet encapsulation.<sup>4</sup> Furthermore, several studies foresee material constraints and environmental challenges associated with the growing demand of the PV industry for base metals such as Cu, Al, and Fe/steel.<sup>27,28</sup> These materials are used for “peripheral” components like the electrical wiring, mounting, and frame and can therefore be regarded as nearly independent of the specific PV technology.

In this work, we exclusively focus on the functional layers of the solar cell stack. As depicted in the inset in [Figure 1A](#), a tandem device consists of top and bottom solar cells to selectively absorb parts of the solar spectrum, which are connected by an interconnection layer. Perovskite tandem stacks consist of multiple functional thin films comprising the perovskite photoabsorber as well as contact layers and electrodes for charge extraction. [Figure 1B](#) depicts the material demand for the production of 1 TW<sub>p</sub> of a representative APT stack (see the materials and layer stack inventory in [supplemental information](#) section “materials and layer inventory”).<sup>23,29–31</sup> In this example, overall 30,194 t/TW<sub>p</sub> are needed for multi-TW-scale production and the assessed material demands range in the order of 100 t to 10 kt/a for most materials. For each functional layer, there are many material options, which also depend on the chosen configuration. To account for the many possible realizations of PST and APT devices, we compiled a comprehensive inventory of the demand of the most frequently used materials and solvents for PSC manufacturing for each of the functional layers ([supplemental information](#) section “materials and layer inventory”). [Figures 1C](#) and [1D](#) exemplarily show the annual demand of indium for transparent electrodes and of cesium for perovskites resulting from the PV growth model.

### Supply criticality of minerals for inorganic materials

In the following, we generalize the above assessment by analyzing a broad range of material layers commonly used for perovskite PV devices. For each layer, we identify the inventory of raw materials used and calculate the necessary demand based on compositions and layer thickness of high-performing devices. Note that not all of the displayed materials are used simultaneously in one device, but the presented range of materials allows for the identification of plausible alternatives for critical materials. For example, if the demand for In for transparent electrodes or Au for opaque electrodes is discussed, this refers to devices which are realized with such materials. Yet, such electrodes could also be made, e.g., from fluorine-doped tin oxide (FTO) or Cu, respectively, which in turn would result in the depicted demand of Sn or Cu in the respective categories. For the assessment of specific layer stacks, details on each material can be found in [Tables S1](#) and [S2](#). Different layer thicknesses can be accounted for by a linear scaling of the reference values listed in [Table S6](#).

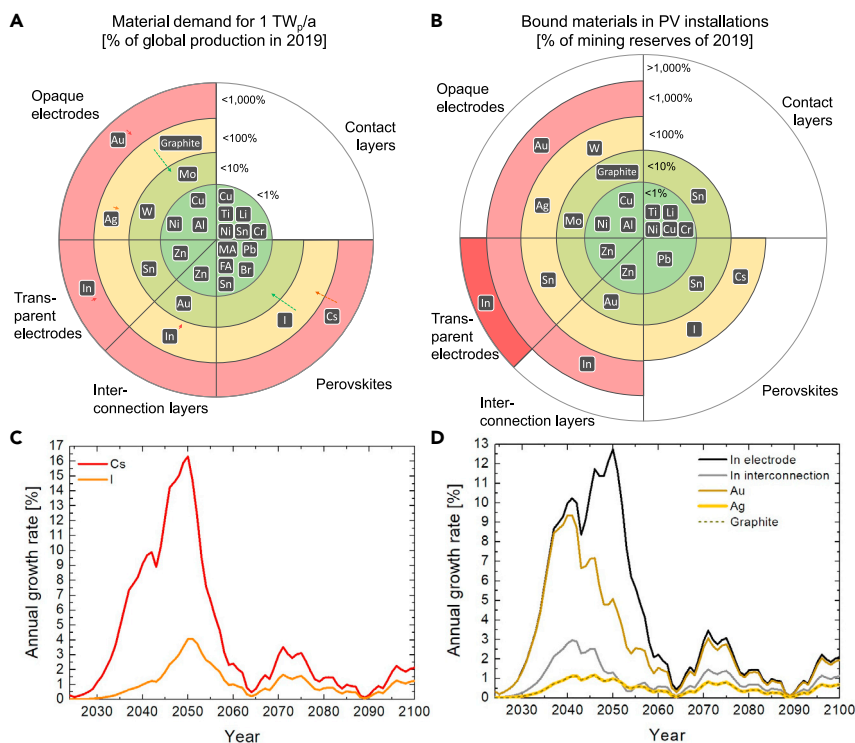


**Figure 2. Material demand for 1 TW<sub>p</sub>/a perovskite PV production and materials bound in multi-TW perovskite PV installations**

(A) Supply risk assessment of inorganic materials used for TW-scale perovskite PV. The figure visualizes the demand-production ratio (DPR) that relates the maximum annual material demand for production of 1 TW<sub>p</sub>/a perovskite modules to the current annual material mining. For comparability, the organic materials methylammonium (MA) and formamidinium (FA) have also been added. Dashed arrows illustrate the potential to reduce the DPR by scaling the production. The underlying material demands were calculated for each functional layer and each material independently, and the materials can be used alternatively, e.g., Cu electrodes would replace an Au electrode. Only for the perovskite absorbers combinations of materials are used as specified in Table S6.

(B) Visualization of the bound-reserves ratio (BRR), relating the materials bound in PV installations with known mining reserves. The BRR of MA, FA, and Br could not be quantified due to unavailable data on reserves.

(C) Necessary annual growth rates of global material production to satisfy the demand for perovskite materials Cs and I. The growth rates for production of Sn, Pb, and Br remain below 0.1%.

(D) Corresponding annual growth rates for production of electrode materials In, Au, Ag, and graphite.

Quantitative values for (A) and (B) are listed in Table S1. A discussion of the material selection is provided in the supplemental information section “materials and layer inventory.”

To evaluate and compare the supply criticality, we apply the demand-production ratio (DPR) typically used in supply risk assessments.<sup>32</sup> The ratio relates the material demand for the production of 1 TW<sub>p</sub>/a PV modules (dashed line in Figures 1C and 1D) to current annual primary production (red solid line). While 1 TW<sub>p</sub> is a useful functional unit that enables comparability between studies, it is important to note that in our model, this figure will be surpassed by a factor of 4 by 2100. Figure 2A summarizes the DPR of the studied inorganic materials (see Table S1 for quantitative values). Most materials have a DPR below or in the range of 1%, which can be considered as not critical in supply, assuming that material production will remain at a comparable level. Given the uncertainties associated with the considered long time-scales, materials with DPR < 10% may also be considered as not critical in supply.

**Box 1. Overview of current production and assessment of future supply of the materials graphite, iodine, silver, gold, indium, and cesium**

The materials have been selected due to a high demand-production ratio (DPR) and bound-reserves ratio (BRR).

**Graphite**

**Occurrence and production:** Graphite consists of crystalline carbon in the form of stacked graphene sheets of various crystalline forms, of which several have been successfully implemented in PSC.<sup>33</sup> Currently, graphite is mostly produced from mining, but can also be fabricated from waste biomass.<sup>34</sup>



**Potential future supply:** Today, around 14% of the global graphite supply is used for anode fabrication in batteries.<sup>35</sup> The International Energy Agency projects a 25-fold increase in global graphite demand by 2040 for the production of batteries for electric vehicles.<sup>36</sup> Despite high projected growth rates of graphite production (6-9%), existing capacities have been assessed to sufficiently satisfy current and future demands.<sup>35</sup> The projected production increase for batteries would lead to a supply 50 times higher than the demand of the perovskite PV industry.

**Assessment of global supply criticality:** Low to medium criticality.

**Substitutes:** Conductive metals, conductive synthetic materials.

**Iodine**

**Occurrence and production:** Iodine is currently produced as by-product in sodium nitrate mines or brines occurring in natural gas production.<sup>25</sup>



**Potential future supply:** The current production of I is comparably low, which is reflected in a DPR of 36.5%, with known reserves<sup>25</sup> resulting in a BRR of 15.3%. While currently not economic, resources might be further expanded by the rich resources of the oceans, containing 90 Gt of I at a concentration of 0.06 ppm.<sup>25</sup> Seaweeds enrich iodine to 0.45%.<sup>25</sup> Brines from water desalination may also become attractive.

**Assessment of global supply criticality:** Medium criticality.

**Substitutes:** None. Iodine is essential for band-gap optimization.

**Silver and Gold**

**Occurrence and production:** Au and Ag are some of the oldest metals used by humans. Mining and exploration are accordingly highly mature.



**Silver supply:** Today, the PV industry consumes approximately one tenth of the global silver production.<sup>4</sup> Provided that the silver market remains unchanged, this renders Ag tolerable for opaque electrode in 1 TW<sub>p</sub>/a of APT perovskite PV, but not for multi-TW production of PST and APT. This is consistent with studies focusing on single-junction silicon PV technologies.<sup>4,37</sup>

**Gold supply:** Considering that Au mining rates might not be able to be increased extensively, gold is not suited as electrode for TW-scale perovskite PV. For completeness, it needs to be added that today, less than 10% of Au mining is used for technological applications and, likewise, large gold stocks are held by central banks. This makes it at least theoretically conceivable that Au is withdrawn from these uses to produce some TW<sub>p</sub> of perovskite PV over a limited time. Yet, this appears to be an unlikely scenario as gold electrodes are too costly for competitive PV modules.<sup>38</sup>

**Gold recycling:** The use of nanometer-thin Au as interconnection layers is likely feasible from a supply perspective (DPR: 2.0%). However, it may be connected to high dissipation losses (64 t/TW<sub>p</sub>) if it is not effectively recycled. In a best case scenario where 1-nm Au is deposited on a module with 2 mm glass/foil module, the Au concentration in the module is approximately 4 g per ton of waste, which is 38 times lower than the Au content in a smart phone (150 g/t), but at the same level as in gold mines.<sup>39</sup> However, as collection and separation have to be considered as cost factor as well, partial recycling of such thin gold layers may only be economic if the gold layer can be separated in a way that enables Au-concentration during recycling. Eventually, the profitability of Au-recycling will depend on the revenues of other recycled materials.

**Assessment of global supply criticality:** High criticality.

**Substitutes:** Conductive metals such as Cu, Al, Ni. Graphite. For interconnection layers, e.g., heterojunctions from electron and hole transport layers, or transparent conductive oxides.

**Indium**

**Occurrence and production:** Indium is mainly used as transparent conductive oxide in display production, typically as indium tin oxide (ITO—90%–95% of In<sub>2</sub>O<sub>3</sub> alloyed with 5%–10% SnO<sub>2</sub>).<sup>24,25</sup> The statistical concentration of indium in the earth's crust is comparable to Ag. However, in contrast to the more common silver-minerals, there are only 12 known minerals that contain indium.<sup>24</sup> Due to the low concentration in ores, In is therefore only extracted as by-product, typically as a trace constituent from sulfate minerals, mainly zinc-sulfate.<sup>25</sup> Indium mining is hence tightly coupled to the mining rates of base metals, the exclusive extraction of indium is not economic.<sup>40</sup> The demand of In for transparent electrodes exceeds the current production by a factor of 2 to 4.5 for perovskite/silicon tandems (PSTs) or all-perovskite tandems (APTs), respectively. For interconnection layers, the DPR is 40% and 30%, respectively.



**Potential future supply:** Interpolating from reserves of the base metals zinc and copper, the global indium reserves have been estimated to 18.8 kt (15.0 kt for Zn alone).<sup>24,41</sup> This results in a BRR of 1,809% for transparent electrodes and 118% for interconnection layers.

**Assessment of global supply criticality:** High criticality for transparent electrodes, medium to high criticality for interconnection layers.

**Substitutes:** For transparent electrodes, e.g., aluminum-doped zinc oxide (AZO), fluorine-doped tin oxide (FTO), PEDOT:PSS. For interconnection layers, e.g., heterojunctions from electron and hole transport layers.

**Cesium**

**Occurrence and production:** The statistical occurrence in the earth crust (3 ppm) is comparable to Sn.<sup>42</sup> However, Cs (as well as Rb) belongs to the large-ion lithophile elements. Due to a large ion radius in combination with comparably low ion potential, it is counted as "incompatible element" and crystallizes only in few minerals, which renders it highly dispersed,<sup>43</sup> with only one important economical



**Box 1. Continued**

source mineral being the rarely occurring pollucite.<sup>42</sup> The current global Cs consumption is low and estimated to be 50 t/a at the most, resulting in a correspondingly low production.<sup>42</sup>

**Potential future supply:** Considering the known reserves of below 200 kt,<sup>25</sup> with a BRR of 12.1% a scale-up of production is conceivable if the production can be scaled rapidly enough.<sup>16</sup> Today, the Cs market is small and Cs is mainly used for drilling in petroleum exploration.<sup>25</sup> In a post-fossil world, this share may be used for perovskite PV. However, this potential market shift will not be able to offset the high demand for Cs from perovskite PV production as Cs demand for 1 TW<sub>p</sub>/a perovskite PV requires a 5-fold increase of the current production (DPR: 561%). Even if the Cs content of the perovskite is reduced from the assumed 20% to only 1%, the demand for 1 TW<sub>p</sub>/a amounts to 28.9% of the current production (see [Table S12](#)). Multi-TW scale PV hence requires even larger increases of Cs mining with annual growth rates as high as 16.3% (see [Figure 2C](#)), which requires a far-sighted establishment of supply chains.

**Substitutes:** Methylammonium or formamidinium. Cs-free APTs have been successfully demonstrated.<sup>44</sup>

A high risk for supply criticality (see discussion in [Box 1](#)) is identified for three materials with a DPR above 100%, namely Au (DPR, 195%), and In used in electrodes (DPR, 457% for APT) and for Cs used in perovskite absorbers (DPR, 561%).

Furthermore, a potentially critical DPR range of 10%–100% is found for the electrode materials graphite (DPR, 13.1%) and Ag (DPR, 13.2%), In in interconnection layers (DPR, 40% for PST, 30% for APT), and I (DPR, 36.5%) in perovskites. Categorizing these materials as critical in supply requires a more detailed assessment of the current and future primary production. As detailed in [Box 1](#), it is likely that the supplies of graphite and iodine will be sufficiently scalable. Silver consumption remains in the same range as the demand of today's PV industry for 1 TW<sub>p</sub> perovskite PV, but the demand is exceeded to potentially critical levels for projected multi-TW production. Note that values for one planar opaque rear electrode are considered here, which is applicable for APT, but not for PST, where an additional semitransparent electrode grid on the front is required, which currently is based on Ag in commercial Si-PV modules.<sup>37</sup> Based on the projections of the Ag-demand of silicon solar cells (front and rear), for PST the consumption could increase by up to a factor of 2.88 ([supplemental information](#) section "materials and layer inventory"), which would raise Ag consumption to critical levels.

Indium demand for interconnection layers with thicknesses of 20–25 nm may also become critical.

Using our PV capacity-expansion model, we also assess the bound-reserves ratio (BRR). This ratio relates the material assets that are bound in global PV installations to the known reserves of the respective material. In [Figures 1C](#) and [1D](#), we indicate the bound materials by the shaded green area and the known reserves with the dark red area. [Figure 2B](#) shows a similar behavior of DPR and BRR, but there are also exceptions: due to relatively larger reserves, the BRR is significantly lower than the DPR for graphite (3.3%) and Cs (12.1%). In contrast, limited reserves lead to an even higher BRR compared with the DPR for the Sn in transparent electrode materials (18.0%) and indium (1,809% for electrodes, 118% for interconnection layers). There is also a higher BRR for electrode materials Au (904%), Ag (52.1%), and W (14.1%). Overall, the consideration of the BRR supports the assessment of a high supply criticality for Au, In, and Ag.

Cesium supply criticality requires a closer investigation, as further discussed in [Box 1](#). There are currently very few applications for Cs which renders the global demand and hence production low. This is reflected in a high DPR. In contrast, the comparably high Cs reserves indicate that an increase in Cs mining may be feasible.<sup>16</sup> It is instructive to assess the necessary annual growth rates of the mining industry to satisfy the material demand for perovskite PV ([Figures 2C](#) and [2D](#)). Note that this

representation does not consider the changing demand of other industries. In our model, the Cs mining needs to be expanded throughout the considered time frame. The expansion is especially rapid until 2050, where the highest annual growth rate of 16.3% is reached. In conclusion, there is a high supply risk for Cs, which may be amended by a far-sighted expansion of the supply chain.

The necessary annual growth rates also allow for assessing the supply criticality of the remaining materials: Iodine is an irreplaceable essential material for perovskite PV. Considering the sufficient time horizon until 2050 when the annual growth rate reaches up to 4.1%, it may be feasible to establish the necessary supply chains. This also applies to graphite with a maximum growth rate of 1.2%.

### Supply criticality of synthetic materials

For advanced synthetic materials—like organic materials, which mainly consist of carbon and hydrogen atoms—just considering the elemental availability is not sufficient, but also the complexity of the synthesis and current technological readiness of industrial production need to be assessed. The scalability of synthetic materials is discussed in the following. Quantitative values are listed in [Table S2](#), and detailed analysis can be found in the [supplemental information](#) section “[production and reserves of minerals](#).”

#### MA and FA halides

Methylammonium (MA<sup>+</sup>) and formamidineium (FA<sup>+</sup>) are essential monovalent cations for perovskites. MA halides are synthesized by the reaction of halide acids and methylamine, which is synthesized from the highly abundant base chemicals methanol and ammonia (current production [CP] > 100 Mt/a). FA halides can be synthesized from FA acetate, which is produced by the reaction of cyanamide (CP > 1 Mt/a) in acetic acid (CP > 10 Mt/a).<sup>45</sup> Therefore, from the perspective of base material production, MA and FA halides production for multi-TW-scale perovskite PV is not critical as base material production exceeds the demand by a factor of 10<sup>6</sup> or 10<sup>5</sup>, respectively.

2D perovskite passivation layers are frequently employed for surface passivation of the photo absorber layer which can be formed from a wide range of large cation halide salts.<sup>46</sup> We selected *n*-octylammonium iodide (OAI) as a representative material, which is employed in highly efficient PSCs.<sup>47</sup> OAI can be easily synthesized by reaction of the common industry chemicals HI acid and octylamine ([Figure S5](#)). Therefore, as for MA and FA halides, we consider the production of OAI and comparable salts as scalable.

#### Organic HTMs

Currently, most organic HTMs employed in high-efficiency PSCs, such as spiro-OMeTAD (53.9% of all published PSCs) ([Table S5](#)), PTAA (5.1%), or P3HT (2.4%), require Pd-based catalyzers during synthesis and are currently only produced for research. For spiro-OMeTAD, we assessed a global annual production of 7.8 kg/a ([Table S9](#)). To satisfy the HTM demand of 100, 1,320, and 1,430 t/a/TW<sub>p</sub> production using PTAA, P3HT, or spiro-OMeTAD, respectively, HTM production would need to be expanded drastically (12,800, 168,955, or 182,778 times, respectively) ([Figure 3A](#)). With a CP of 227 t of palladium, mainly used for combustion engines, Pd supply likely represents no risk for the scaling in production of these HTMs. However, these HTMs can currently be synthesized only in gram-sized batches with a low yield (17.8% for spiro-OMeTAD, 43.2% for PTAA), long synthesis durations (>45 h for spiro-OMeTAD, >12 h for PTAA), and complex production routes (7 steps for

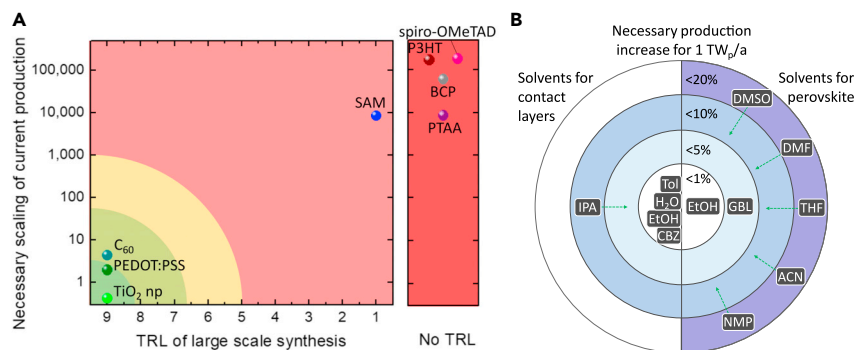


**Figure 3. Required increase of production for synthetic contact materials and solvents**

(A) Necessary scaling of production and increase in technological readiness level (TRL) of the industrial synthesis of synthetic materials for 1 TW<sub>p</sub>/a perovskite PV production. No TRL means that no technological concept for industrial production has been formulated yet.

(B) Necessary increment of solvent production for the production of 1 TW<sub>p</sub>/a perovskite PV. Dashed arrows illustrate potential to reduce consumption by solvent recycling.

spiro-OMeTAD, 4 steps for PTAA) requiring various educts, solvents, and acids.<sup>48,49</sup> If these HTMs are to be employed for multi-TW-scale perovskite PV production, research on industrial synthesis needs achieve major step-changes.

Bathocuproine (BCP) is a common buffer layer in p-i-n PSCs between the electron transport layer such as fullerenes and the metal back electrode.<sup>23,29,30,50</sup> The synthesis of BCP involves four reaction steps with 14 different reactants and has an overall yield of 59% (see supplemental information section “materials and layer inventory” for more details). Since the synthesis involves a Pd-catalyzed coupling reaction, as for the HTMs discussed above, we consider it highly challenging to scale up the synthesis of BCP to the levels of t/a or kt/a.

Self-assembled monolayers (SAMs), like 2PACz are the HTMs that yield highest efficiencies in tandem PSC.<sup>7,30,31</sup> These materials are currently still expensive to produce. However, they differ from other HTMs as only a molecular monolayer of approximately 1 nm thickness is needed. Considering the known synthesis routes, we estimate that the production is principally scalable to the amount of 67 t/a which is necessary for 1 TW<sub>p</sub>/a perovskite PV. What remains beyond the scope of this work is a detailed assessment of the supply or scalability or substitutability of the necessary educts, especially laboratory-type chemicals.

PEDOT:PSS is an exception among organic HTMs as industrial production is already well established for automotive as well as consumer applications. A PEDOT:PSS production of 200 t/a is necessary to fabricate 1 TW/a of perovskite PV, which would correspond to approximately 10,000 t/a of dispersion. Based on our knowledge of the industrial landscape, we estimate that material production at this scale is feasible but might require additional production capacity.

### Fullerenes

The industrial production of fullerenes (e.g., C<sub>60</sub> or PCBM), which are used as electron-transport layer, has already been scaled to an annual production in the multi-ton range. Consequently, although there is a considerable degree of uncertainty about the precise production volume, reaching the demand of 220 t/a/TW<sub>p</sub> for APT solar cell stacks appears to be feasible from a material supply perspective (see supplemental information section “production and reserves of minerals” for detailed discussion).

### TiO<sub>2</sub> nanoparticles

Most of the high-efficiency single-junction PSCs contain a hole-blocking compact layer of titania (c-TiO<sub>2</sub>) and an electron-selective mesoporous titania (m-TiO<sub>2</sub>) (Table S5). These materials are produced by different methods from a common precursor of TiCl<sub>4</sub>, which can be either combined with isopropanol to produce titanium isopropoxide for the deposition of c-TiO<sub>2</sub>, or used for synthesis of TiO<sub>2</sub> nanoparticles by the flame-spray pyrolysis method,<sup>51</sup> from which the m-TiO<sub>2</sub> layer is later fabricated. TiCl<sub>4</sub> is typically synthesized from the most common Ti-ore ilmenite (FeTiO<sub>3</sub>), which is mined at a rate of 7.6 Mt/a,<sup>25</sup> corresponding to a DPR of 0.049%. TiO<sub>2</sub> particles have been used for paints and inks for decades, highlighting the maturity of TiO<sub>2</sub>-np industry. Today, the TiO<sub>2</sub>-np production of 3 kt<sup>52</sup> already surpasses the demand (1.9 kt) for 1 TW/a of APT solar cell stacks.

### Solvents

A key appeal of PSCs is that most of the functional layers can be dissolved and processed in liquid form. For perovskites absorbers, the most common solvent are blends of dimethylformamide (DMF) and dimethyl sulfoxide (DMSO).<sup>53</sup> Notable alternatives are N-methylpyrrolidone (NMP) and  $\gamma$ -butyrolactone (GBL).<sup>53</sup> Recently, highly volatile solvents with faster evaporation rates have been considered for large scale deposition such as acetonitrile (ACN), ethanol (EtOH), or tetrahydrofuran (THF).<sup>54</sup> For contact layers, most common solvents are toluene (Tol), chlorobenzene (CB), EtOH, isopropyl alcohol (IPA), or H<sub>2</sub>O. Figure 3B compares the solvent demand for 1 TW<sub>p</sub>/a with the current production, demonstrating that there is sufficient solvent production for contact layers, but a manageable scale-up of up to 20% may be necessary for the additional demand for perovskite absorber deposition. Moreover, as discussed in the next section, the consumption may be drastically decreased with onsite solvent recycling. Therefore, we conclude that solvent consumption reaches volumes that require close consideration, but there will be likely enough supply for multi-TW-scale perovskite PV.

### Perovskite PV recycling and material losses

As material demand keeps increasing strongly, only a small part of the material feedstock of the PV infrastructure can be gained by recycling of discarded PV modules, and hence supply strongly depends on primary material production. Nonetheless, the massive material streams in the range of kilotons for individual materials require thorough consideration of dedicated recycling strategies already in the early stages of technology development. Therefore, high recycling efficiencies need to be achieved for end-of-life (EOL) modules and production scrap in all three recycling stages of collection, preprocessing to separate various materials, and end-processing to achieve purified materials (Figure 4).<sup>39</sup>

Measured by mass, the PV industry is by far the largest semiconductor industry. For recycling this can be advantageous because it provides a large and rather homogeneous material base for effective waste management. EOL modules, however, possess a relatively low value-to-weight ratio, which makes collection and preprocessing distance sensitive. On the other hand, strongly reduced capital investment costs for perovskite PV module plants open opportunities for decentralized production.<sup>55</sup> This offers the possibility to establish rather local circular economy material networks.

A key challenge for recycling of silicon PV technologies is that in a module, the silicon wafers are tightly bound to the glass substrate by the encapsulant, typically polyethylene-co-vinyl acetate (EVA), which makes it challenging to recover all materials cost effectively at high purity levels.<sup>56</sup>

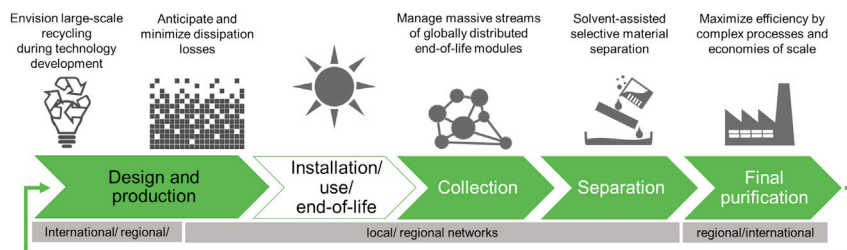


**Figure 4. Guidelines for perovskite PV recycling**

Perovskite PV offers promising advantages for innovative recycling strategies if the challenges of massive waste streams are addressed in early stage of technology research. EOL module recycling is carried out in the three stages of module collection, materials separation, and final purification. The first two stages can, especially, well be embedded in networks of local production, use, and recycling, while less mass-intensive final purification may benefit from centralized economies of scale. Solvent-assisted material separation is promising to increase the concentration yield supplied to final purification stage. In all stages, dissipation losses must be anticipated and minimized.

In contrast, most layers of the PSC stack can be separated and concentrated by low-temperature leaching processes via selective organic solvents,<sup>57</sup> which also opens possibilities for innovative design-for-recycling concepts.<sup>58</sup> This applies especially to inorganic materials. In principle, organic materials can also be recycled from EOL modules since they show different solubility in low polar solvents compared with perovskite, but this might be challenging and uneconomic in practice, as these materials will usually have degraded, e.g., by oxidation. Moreover, as the curing of EVA releases byproducts that can degrade perovskite layers,<sup>59</sup> the development of advanced encapsulants for perovskite PV<sup>59,60</sup> opens the possibility to implement novel approaches where the encapsulation does not only provide robust long-term protection during operation but is also optimized for EOL recycling. As we recently demonstrated, this could be realized, for example, by designing the encapsulant as a “release layer” that induces a separation between cell and cover glass upon thermal or wet-chemical activation in the recycling step.<sup>58</sup>

As for solvent recycling during the production phase, recovery rates of 71% have been estimated if the solvents are captured in a condenser and purified in a distillation process.<sup>51</sup> Some materials like transparent conductive oxides (TCOs) cannot be recovered by leaching. If FTO is used as TCO, efficient recycling of FTO glass should be implemented as the BRR for Sn in FTO is 18.0%.

Finally, reducing material consumption is not an unconditionally advantageous strategy for more resource efficiency. Dissipation of minute layer thicknesses on large cumulative module areas may pose a serious challenge for the goal of a circular economy. For example, thin 1-nm layers of gold may not be economically recoverable for individual recycling sites and perovskite PV production might globally add up to dissipative gold losses of 64 t/a/TW<sub>p</sub>. Moreover, the entire APT infrastructure would bind up to 4.95 kt of Au, which corresponds to almost 10% of global Au reserves (BRR = 9.3%). Thus, dissipation losses need to be considered in the early stages of research.

## DISCUSSION

Our criticality assessment of lead, iodine, bromine, and indium is in line with findings of other studies that investigated the supply criticality for perovskite PV.<sup>14–16</sup> Also the finding of high criticality for Ag agrees with previous assessments.<sup>15,16,37,62</sup> For cesium, we find a much higher DPR value in comparison with values reported

in a previous study that assessed similar perovskite composition.<sup>16</sup> We attribute this discrepancy to an overestimation of the Cs production in this preceding report. The literature treating Cs production is scarce and there are no official numbers on Cs production.<sup>25</sup> However, the estimates of Cs production used in our study have been confirmed by the US Geological Survey via personal correspondence. Our assessment that the current Cs production is likely especially low because there is a very low demand and that there may be a high potential to scale-up the production is well in line with the preceding report.<sup>16</sup> An important question which requires further research is whether Cs mining can be scaled at the same pace as the growth of the perovskite PV industry. Our assessment of solvent demand per square meter of perovskite PV modules are well in line with the study by Vidal et al. (see further discussion in the [experimental procedures](#)).<sup>61</sup> We are not aware of preceding works assessing the supply criticality of synthetic materials for multi-TW scale perovskite PV.

The material inventory discussed here can be regarded as representative of frequently used materials for perovskite PV devices. Although the supply criticality was discussed using the example of 2-terminal perovskite tandem devices, our assessment can be straightforwardly transferred to other perovskite PV architectures, such as single- or triple-junction devices. To illustrate this further, we briefly discuss the application to a 4-terminal PST device with a PSC stack of FTO/NiO/perovskite/PCBM/BCP/aluminum doped-zinc oxide (AZO)/Ag<sup>63</sup>: all of these layers are tabulated in [Tables S1](#) and [S2](#); the values listed there simply need to be scaled by the specific layer thickness in case it deviated from the one listed in [Table S6](#).

Over the long time frame considered in our study, novel materials will appear that have not been taken into account yet. The inventory of inorganic raw materials is limited by the number of elements in the periodic table, of which several with relevance for optoelectronic applications have already been covered here. In contrast, there are vast possibilities for novel synthetic materials for which the industrial scalability should be considered already in the early stages of material development. We intentionally did not apply further selection criteria to the materials inventory, e.g., by discarding materials that are currently too costly, may induce device degradation, or reduce the solar cell efficiency, as these properties may change with further material development.

Finally, it needs to be kept in mind that all numbers presented here are associated with high uncertainties. For example, resource consumption scales roughly reciprocally with module lifetime ([supplemental information](#) section “[sensitivity analysis of module lifetime](#)”). Moreover, a wide range of scenarios for climate-change-compatible annual PV installation rates to limit climate change exist and higher installation numbers would increase resource demand (by up to a factor of 3 in 2050), while the perseverance of silicon technology or the emergence of other technologies would reduce the demand.

### Conclusions for perovskite PV research

In this study, we assessed the material demand of a multi-TW-scale perovskite tandem PV infrastructure. By comparing the results with current material production, we draw the following conclusions: multi-TW scale perovskite PV is feasible from a material supply perspective; the statement that PSCs are made from “abundant materials” is generally justified. However, especially the materials In, Au, and Cs are associated with high supply criticality as the amounts required for 1 TW<sub>p</sub>/a PSC production represent approximately 200%, 460%, and 560% of CP, respectively. This is a critical finding as current research activities—driven by the paradigm established by the highest performing devices—are highly focused on device architectures that employ these

materials. Indium must be replaced in transport layers, but already the smaller demand from its use in interconnection layers is associated with supply risks. Although there are sufficient known Cs reserves, the necessary growth rates for Cs mining expansion of up to 16.3% per year are ambitious. To reduce supply risks, research needs to investigate the development of stable cesium-free perovskites. This finding is especially critical for the research direction of completely inorganic perovskites as well as for the use of Cs in stable high band-gap perovskite absorbers. If Cs is believed to be necessary for multi-TW-scale perovskite PV production, a far-sighted development of the necessary supply chains is important. Furthermore, Au- and Ag-metal electrodes need to be replaced by abundant base metals such as Cu, Al, or graphite. With the exception of PEDOT:PSS none of the synthesis routes of organic charge transport materials are currently compatible with industrial large-scale production. Pathways for economic upscaling of production need to be urgently researched. On the other hand, inorganic nanoparticle materials have a high technological maturity and low raw material demand compared with current annual production.

The layer thickness and hence absolute material demand of the active perovskite PV devices stack is approximately 200 times lower than that of established Si-based PV devices. Yet, this work demonstrates that, despite using layer thicknesses in the sub-micrometer range, 1 TW<sub>p</sub>/a perovskite PV production implies annual material demands in the range of kilotons for the PSC stack. For the initial build-up of the global PV infrastructure, little of the required material can be withdrawn from existing material stocks within PV, which implies containing or expanding mining activities or the use of other material stocks, e.g., from fossil industries. An important question, which is beyond the scope of this work, is whether the necessary mining rates can be achieved and what will be the implication for humans, the environment, and the planet. Therefore, further works should focus on other aspects of criticality, such as supply chain vulnerability or social and ecological aspects. In any case, the large material stocks aggregated in PV modules and the foreseeable massive material waste streams mandate that researchers adapt a resource sensitivity and a “design-for-recycling” thinking already in the early stages of technology development.

## EXPERIMENTAL PROCEDURES

### Resource availability

#### Lead contact

Further information and requests for resources and materials should be directed to and will be fulfilled by the lead contact, Lukas Wagner ([lukas.wagner@physik.uni-marburg.de](mailto:lukas.wagner@physik.uni-marburg.de)).

#### Materials availability

This study did not generate new unique materials.

#### Data and code availability

Data generated during and analyzed in this study is available in the manuscript or [supplemental information](#). Furthermore, a document containing underlying data and specifying the calculations is available in a public repository at <https://doi.org/10.5281/zenodo.10407137>.

### Expansion scenarios for the PV industry

We use the global multi-regional energy-economy-climate model REMIND Version 2.1.0 for our analysis.<sup>21</sup> REMIND is open source and available on GitHub at <https://github.com/remindmodel/remind>. The technical documentation of the equation structure can be found at <https://rse.pik-potsdam.de/doc/remind/2.1.0/>.

In REMIND, each single region is modeled as a hybrid energy-economy system and is able to interact with the other regions by means of trade. Tradable goods are the exhaustible primary energy carriers coal, oil, gas and uranium, emission permits, and a composite good that represents all other tradable goods. The economy sector is modeled by a Ramsey-type growth model which maximizes utility, a function of consumption. Labor, capital, and end-use energy generate the macroeconomic output, i.e., gross domestic product (GDP). The produced GDP covers the costs of the energy system, the macroeconomic investments, the export of a composite good and consumption.

The energy sector is described with high technological detail. It uses exhaustible and renewable primary energy carriers and converts them to final energy types such as electricity, heat, and fuels. Various conversion technologies are available, including technologies with carbon capture and storage (CCS). The model includes cost mark-ups for the fast upscaling of investments into individual technologies; therefore, a more realistic phasing in and out of technologies is achieved.

The scenario used in this paper follows the default settings of the model, which were also used for scenario S1 in our earlier study.<sup>4</sup> To match the historic standing capacity data in the year 2020, 47 GW<sub>p</sub> were added to the REMIND data in each year. Furthermore, the REMIND model delivers the cumulative installed PV capacity in time steps of 5 years until 2060 and in time steps of 10 years until 2100. To obtain data with a yearly resolution, in a first step preliminary installed PV capacity data was estimated for the intermediate years using the CAGR calculated for the 5- or 10-year time period. Lower CAGR values in a following time period then sometimes lead to a sharp drop in the annual active capacity expansion, when going from one time period to the next. To avoid these artificial oscillations, the data for the annual active capacity expansion was smoothed by a moving average over  $\pm 4$  years. Finally, by integrating over these values and smoothing with a moving average over  $\pm 1$  year we obtained the data for the installed PV capacity data without implausible jumps at the transition between time periods, which is used in the present study. While there is a certain discrepancy in the transition from the historic to the projected data, after 2025 the deviation from the REMIND data-points lies below 2.7%. The discrepancy decreases steadily and is below 1% from 2045 on. Respective data for annual active capacity expansion was calculated from the difference in installed PV capacity to the previous year.

To account for the module lifetime  $\tau$  of 25 years, the PV production in year  $t$ ,  $P^r(t)$ , is calculated from the sum of the active capacity expansion in the same year  $P(t)$  and the production from  $\tau$  years ago by

$$P^r(t) = P(t) + P^r(t - \tau) \quad (\text{Equation 1})$$

### Modeling of perovskite PV market shares

As the PV market is dominated by silicon PV, it is likely that the first tandem PV modules to enter the market will use silicon as bottom cell.<sup>64</sup> Once perovskite PV technology is industrially established via PSTs, it is plausible to assume that the market will move toward APT and multi-junction devices to unravel the full potential of the perovskite technology. This study focuses on tandem (two junction) cells. Even higher power conversion efficiencies can be reached with a larger number of junctions.<sup>65</sup> However, it is difficult to speculate on the future development of multi-junction perovskite PV such as the market entry and number of junctions. The material demand for devices with more junctions can be interpolated from our assessment,

considering that the number of layers will increase. Thereby, it can be assumed that, except for the perovskite layer, the material compositions and layer thicknesses will be not be fundamentally altered.<sup>66,67</sup>

To model the market entry of new perovskite technologies, logistic growth was assumed to the annual production of the new technology  $P_{new}$  in year  $t$

$$P_{new}(t) = \frac{P_{tot}(t)}{1 + e^{-k \cdot (t - t_0)}} \quad (\text{Equation 2})$$

Herein,  $P_{tot}(t)$  is the total PV production in year  $t$ ,  $k$  describes the growth rate.  $t_0$  marks the time when 50% of market share is reached. We assumed that for PST devices,  $t_0$  will be reached in 2040, and in 2050 for APTs. A discussion of the assumptions underlying the perovskite PV growth model is detailed in [supplemental information](#) section “[further details on the perovskite PV industry growth model.](#)”

### Plausibility of assumed growth rate

In [Equation 2](#),  $k$  is a factor that describes the growth rate, which was set to 0.36 for PST PV to be in line with the projections of the International Roadmap for Photovoltaic.<sup>6</sup> Comparing with historic data, this can be considered as a conservative estimate. For comparison, between 2016 and 2020, the growth of the market share of monocrystalline silicon PV to the total PV market could be fit by a logistic growth curve with a growth factor  $k$  of 0.6 ([Figure S2](#)). We chose a considerably lower value as monocrystalline silicon PV was already an established technology by 2016. Likewise, a slightly higher growth factor of 0.4 was assumed for APTs to account for the fact that by that time, technological readiness of perovskite PV technologies will be industrially mature, however, only for coating sizes of silicon wafers whereas large scale thin film coating techniques still need to come to maturity.

### Module area determination

To assess the produced module area, first the annual PV module capacity addition was calculated from the installed capacity estimated by the REMIND model. With the annual module efficiency, projected with an efficiency learning rate of 7.9% for each doubling of the cumulative module production, this yields the annual produced module area. For the reference of 1 TW<sub>p</sub>/a module production, a module efficiency of 30% was assumed. This is an arbitrary, but representative value (reached by 2053 in our model) which results in a module production of  $3.33 \cdot 10^9$  m<sup>2</sup>/a.

### Materials inventory and layer thicknesses

A detailed discussion of the selection of considered materials can be found in [supplemental information](#) section “[materials and layer inventory.](#)” The material demand is governed by the required layer thickness. In specific solar cell stacks, these thicknesses are optimized to yield the optimal device performance. Therefore, it is not possible to assign to a specific material a definite layer thickness. In this study, we considered the layer thicknesses of the latest laboratory efficiency records or of other high-performing device stacks to represent a well-optimized system. It is reasonable to assume that, although the layer thickness of future optimized device stacks may vary, the concrete numbers may not differ by orders of magnitudes, which is the core focus of the present supply criticality assessment. The layer thicknesses used for the assessment are listed in [Table S6](#).

### Assessment of solid materials demand

The material demand of solid material is listed in [Table S1](#). For APTs, the material consumption of contact layers assumes that the respective layer is used twice,

once in the top and once in the bottom cell. For inorganic materials, the consumption of the mass of elemental materials per unit area was computed. Therefore, the effective density of each element in the respective material was calculated (e.g., Pb in perovskite). For perovskite blends, material densities were assessed by a linear interpolation between reported values of perovskite compounds.

### Assessment of solvent demand

For the assessment of the solvent demand of perovskite precursors, first the solvent demand to coat the targeted layer thicknesses was estimated based on precursor concentrations reported in the respective publications referenced in [Table S6](#). Spilling losses during deposition were not considered. For PSTs, this yields a demand of 1.79 mL/m<sup>2</sup> DMF and 0.446 mL/m<sup>2</sup> DMSO. The formation of the two perovskite layers in the APT architecture requires 6.07 mL/m<sup>2</sup> DMF and 1.03 mL/m<sup>2</sup> of DMSO, i.e., the total solvent demand is 7.09 mL/m<sup>2</sup>. For a direct comparison between different solvents, we set the solvent demand to 7 mL/m<sup>2</sup> for all solvents. This is in accordance to the assessment by Vidal et al.<sup>61</sup> who assumed 2.5 mL/m<sup>2</sup>, considering that they studied single-junction devices which contain only one perovskite layer and have lower layer thicknesses than the perovskite layers in APT devices. For APT devices, two layers—one for each subcell—of each contact layer were assumed in our calculation.

To assess the solvent demand for contact layers, concentrations of 2 mg/mL PTAA in Tol,<sup>23</sup> 0.375 mg/mL SAM in EtOH,<sup>23</sup> 90.9 mg/mL spiro-OMeTAD in CB,<sup>68</sup> and 10 mg/mL PCBM in CB<sup>69</sup> were assumed, taking representative literature values as a basis. To also include isopropanol in the study, the same solvent demand as estimated for EtOH was assumed.

### Assessment of material supply

Data on supply and reserves for inorganic materials were obtained from publications of the United States Geological Survey<sup>25</sup> unless otherwise noted (see [Table S7](#)). [Supplemental information](#) section “[production and reserves of minerals](#)” comprises a comprehensive discussion of synthesis routes for synthetic solid materials. Numbers for annual solvent production are listed in [Table S11](#).

### Annual growth rate

The annual growth rates  $R$  in a year  $t$  indicates the necessary growth rates of the material production  $M(t)$  within one year,  $R(t) = \frac{M(t) - M(t-1)}{M(t-1)}$ . The expression assumes that the material demand for other uses remains constant at the level of material production of 2019,  $M^{\text{base}}(2019)$ , (see [Table S7](#)) whereas only the demand for applications in perovskite PV,  $M^{\text{perovskite}}(t)$ , changes, i.e.,  $M(t) = M^{\text{perovskite}}(t) + M^{\text{base}}(2019)$ . Annual growth rates of the synthetic materials spiro-OMeTAD, PTAA, P3HT, and SAM as well as PEDOT:PSS, C<sub>60</sub> and TiO<sub>2</sub> nanoparticles are reported in [supplemental information](#) section “[annual growth rates of selected materials](#).”

### Sensitivity analysis

A sensitivity analysis for the materials cesium and indium, identified as supply critical in this study, have been carried out in [supplemental information](#) sections “[sensitivity analysis of cesium demand](#)” and “[sensitivity analysis of cesium demand](#),” respectively. A sensitivity analysis of the effect of the module lifetime on material demand can be found in [supplemental information](#) section “[sensitivity analysis of module lifetime](#).”

## SUPPLEMENTAL INFORMATION

Supplemental information can be found online at <https://doi.org/10.1016/j.joule.2024.01.024>.

## ACKNOWLEDGMENTS

The work on this publication was supported by European Union's Horizon Europe Framework Programme for research and innovation under grant agreement no. 101084124 (DIAMOND). J.S. acknowledges the funding from the Swiss National Science Foundation for financial support with project no. 200020\_185041. The authors acknowledge the valuable revisions of Christian Hagelüken (Umicore AG & Co KG), especially concerning the discussion of recycling, Wilfried Lövenich (Heraeus Deutschland GmbH & Co KG) for valuable contributions to the assessment of PEDOT:PSS supply, and Sebastiano Bellani (BeDimensional S.p.A.) for valuable discussions on production of synthetic materials, especially fullerenes. The authors thank Nils Langlotz (University of Marburg) for his help with the assessment of solvent demands, Michael Daub (University of Freiburg) for providing data of perovskite densities, and Cris C. Tuck (USGS) for valuable feedback on Cs production.

## AUTHOR CONTRIBUTIONS

L.W. and J.C.G. conceived the research question; L.W. assembled the data, conducted the calculations, and coordinated the cooperation; L.W. and R.P. developed the perovskite PV capacity expansion model; L.W. assessed the supply criticality of inorganic compounds; J.S., B.Y., D.B., and L.W. assessed the supply criticality of synthetic material; L.W. conceived the discussion of perovskite PV recycling and material losses; L.W., J.C.G., A.G., and E.G. analyzed the results and assessments of supply criticality; L.W. wrote the manuscript and [supplemental information](#). J.C.G. revised and improved the manuscript and [supplemental information](#). All authors reviewed the final manuscript and [supplemental information](#).

## DECLARATION OF INTERESTS

D.B. is currently an employee of Solarlab Aiko Europe GmbH.

Received: June 12, 2023

Revised: October 23, 2023

Accepted: January 25, 2024

Published: February 27, 2024

## REFERENCES

- Breyer, C., Khalili, S., Bogdanov, D., Ram, M., Oyewo, A.S., Aghahosseini, A., Gulagi, A., Solomon, A.A., Keiner, D., Lopez, G., et al. (2022). On the history and future of 100% renewable energy systems research. *IEEE Access* 10, 78176–78218.
- IPCC (2022). Mitigation of climate change. Contribution of Working Group III to the Sixth Assessment Report of the Intergovernmental Panel on Climate Change (2022) (IPCC).
- Haegel, N.M., Atwater, H., Barnes, T., Breyer, C., Burrell, A., Chiang, Y.M., de Wolf, S., Dimmler, B., Feldman, D., Glunz, S., et al. (2019). Terawatt-scale photovoltaics: transform global energy. *Science* 364, 836–838.
- Goldschmidt, J.C., Wagner, L., Pietzcker, R., and Friedrich, L. (2021). Technological learning for resource efficient terawatt scale photovoltaics. *Energy Environ. Sci.* 14, 5147–5160.
- Richter, A., Hermle, M., and Glunz, S.W. (2013). Reassessment of the limiting efficiency for crystalline silicon solar cells. *IEEE J. Photovolt.* 3, 1184–1191.
- ITRPV (2022). International technology roadmap for photovoltaic, Thirteenth Edition (ETIP Photovoltaics).
- Al-Ashouri, A., Köhnen, E., Li, B., Magomedov, A., Hempel, H., Caprioglio, P., Márquez, J.A., Morales Vilches, A.B., Kasparavicius, E., Smith, J.A., et al. (2020). Monolithic perovskite/silicon tandem solar cell with 29% efficiency by enhanced hole extraction. *Science* 370, 1300–1309.
- Mariotti, S., Köhnen, E., Scheler, F., Sveinbjörnsson, K., Zimmermann, L., Piot, M., Yang, F., Li, B., Warby, J., Musiienko, A., et al. (2023). Interface engineering for high-performance, triple-halide perovskite–silicon tandem solar cells. *Science* 381, 63–69.
- Chin, X.Y., Turkay, D., Steele, J.A., Tabean, S., Eswara, S., Mensi, M., Fiala, P., Wolff, C.M., Paracchino, A., Artuk, K., et al. (2023). Interface passivation for 31.25%-efficient perovskite/silicon tandem solar cells. *Science* 381, 59–63.
- Aydin, E., Ugur, E., Yildirim, B.K., Allen, T.G., Dally, P., Razaq, A., Cao, F., Xu, L., Vishal, B., Yazmaciyan, A., et al. (2023). Enhanced optoelectronic coupling for perovskite-silicon tandem solar cells. *Nature* 623, 732–738.

11. Wagner, L., Mastroianni, S., and Hinsch, A. (2020). Reverse manufacturing enables perovskite photovoltaics to reach the carbon footprint limit of a glass substrate. *Joule* 4, 882–901.
12. Vidal, R., Alberola-Borràs, J., Sánchez-Pantoja, N., and Mora-Seró, I. (2021). Comparison of perovskite solar cells with other photovoltaics technologies from the point of view of life cycle assessment. *Adv. Energy Sustain. Res.* 2, 2000088.
13. Roffeis, M., Kirner, S., Goldschmidt, J.-C., Stannowski, B., Perez, L.M., Case, C., and Finkbeiner, M. (2022). New insights into the environmental performance of perovskite-on-silicon tandem solar cells – a life cycle assessment of industrially manufactured modules. *Sustainable Energy Fuels* 6, 2924–2940.
14. Ball, J.M., and Petrozza, A. (2016). Defects in perovskite-halides and their effects in solar cells. *Nat. Energy* 1, 16149.
15. Wang, L., Zhang, Y., Kim, M., Wright, M., Underwood, R., Bonilla, R.S., and Hallam, B. Sustainability evaluations on material consumption for terawatt-scale manufacturing of silicon-based tandem solar cells. *Prog. Photovolt. Res. Appl.* 31, 1442–1454.
16. Kamaraki, C., Klug, M.T., Green, T., Miranda Perez, L., and Case, C. (2021). Perovskite/silicon tandem photovoltaics: technological disruption without business disruption. *Appl. Phys. Lett.* 119, 070501.
17. Xiao, Z., Yuan, Y., Shao, Y., Wang, Q., Dong, Q., Bi, C., Sharma, P., Gruverman, A., and Huang, J. (2015). Giant switchable photovoltaic effect in organometal trihalide perovskite devices. *Nat. Mater.* 14, 193–198.
18. Huang, J., Yuan, Y., Shao, Y., and Yan, Y. (2017). Understanding the physical properties of hybrid perovskites for photovoltaic applications. *Nat. Rev. Mater.* 2, 17042.
19. Qin, P., Tanaka, S., Ito, S., Tetreault, N., Manabe, K., Nishino, H., Nazeeruddin, M.K., and Grätzel, M. (2014). Inorganic hole conductor-based lead halide perovskite solar cells with 12.4% conversion efficiency. *Nat. Commun.* 5, 3834.
20. Li, Z., Klein, T.R., Kim, D.H., Yang, M., Berry, J.J., van Hest, M.F.A.M., and Zhu, K. (2018). Scalable fabrication of perovskite solar cells. *Nat. Rev. Mater.* 3, 18017.
21. Baumstark, L., Bauer, N., Benke, F., Bertram, C., Bi, S., Gong, C.C., Dietrich, J.P., Dirnaichner, A., Giannousakis, A., Hilaire, J., et al. (2021). REMIND2.1: transformation and innovation dynamics of the energy-economic system within climate and sustainability limits. *Geosci. Model Dev.* 14, 6571–6603.
22. Philipps, S., and Warmuth, W. (2022). Photovoltaics Report. <https://www.ise.fraunhofer.de/content/dam/ise/de/documents/publications/studies/Photovoltaics-Report.pdf>.
23. Abdollahi Nejad, B., Ritzer, D.B., Hu, H., Schackmar, F., Moghadamzadeh, S., Feeney, T., Singh, R., Laufer, F., Schmager, R., Azmi, R., et al. (2022). Scalable two-terminal all-perovskite tandem solar modules with a 19.1% efficiency. *Nat. Energy* 7, 620–630.
24. Gunn, G. (2014). *Critical Metals Handbook* (John Wiley & Sons; American Geophysical Union).
25. U.S. Geological Survey (2021). Mineral Commodity Summaries. <https://doi.org/10.3133/mcs2021>.
26. Tandemzellen-Produktion Oxford PV <https://www.oxfordpv.com/de/tandemzellen-produktion>.
27. Lennon, A., Lunardi, M., Hallam, B., and Dias, P.R. (2022). The aluminium demand risk of terawatt photovoltaics for net-zero emissions by 2050. *Nat. Sustain.* 5, 357–363.
28. Underwood, R., Kim, M., Drury, S., Zhang, Y., Wang, L., Chan, C., and Hallam, B. (2023). Abundant material consumption based on a learning curve for photovoltaic toward net-zero emissions by 2050. *Sol. RRL* 7, 2200705.
29. Lin, R., Wang, Y., Lu, Q., Tang, B., Li, J., Gao, H., Gao, Y., Li, H., Ding, C., Wen, J., et al. (2023). All-perovskite tandem solar cells with 3D/3D bilayer perovskite heterojunction. *Nature* 620, 994–1000.
30. Lin, R., Xu, J., Wei, M., Wang, Y., Qin, Z., Liu, Z., Wu, J., Xiao, K., Chen, B., Park, S.M., et al. (2022). All-perovskite tandem solar cells with improved grain surface passivation. *Nature* 603, 73–78.
31. Chen, H., Maxwell, A., Li, C., Teale, S., Chen, B., Zhu, T., Ugur, E., Harrison, G., Grater, L., Wang, J., et al. (2023). Regulating surface potential maximizes voltage in all-perovskite tandems. *Nature* 613, 676–681.
32. Helbig, C., Bruckler, M., Thorenz, A., and Tuma, A. (2021). An overview of indicator choice and normalization in raw material supply risk assessments. *Resources* 10, 79.
33. Bogachuk, D., Tsuji, R., Martineau, D., Narbey, S., Herterich, J.P., Wagner, L., Suginuma, K., Ito, S., and Hinsch, A. (2021). Comparison of highly conductive natural and synthetic graphites for electrodes in perovskite solar cells. *Carbon* 178, 10–18.
34. Purkait, T., Singh, G., Singh, M., Kumar, D., and Dey, R.S. (2017). Large area few-layer graphene with scalable preparation from waste biomass for high-performance supercapacitor. *Sci. Rep.* 7, 15239.
35. Damm, S., and Zhou, Q. (2020). Supply and demand of natural graphite. *DERA Rohst* 43, 36.
36. International Energy Agency (2021). *The Role of Critical Minerals in Clean Energy Transitions* (International Energy Agency).
37. Hallam, B., Kim, M., Zhang, Y., Wang, L., Lennon, A., Verlinden, P., Altermatt, P.P., and Dias, P.R. (2023). The silver learning curve for photovoltaics and projected silver demand for net-zero emissions by 2050. *Prog. Photovolt. Res. Appl.* 31, 598–606.
38. Song, Z., McElvany, C.L., Phillips, A.B., Celik, I., Krantz, P.W., Waththage, S.C., Liyanage, G.K., Apul, D., and Heben, M.J. (2017). A technoeconomic analysis of perovskite solar module manufacturing with low-cost materials and techniques. *Energy Environ. Sci.* 10, 1297–1305.
39. Hagelüken, C., and Goldmann, D. (2022). Recycling and circular economy—towards a closed loop for metals in emerging clean technologies. *Miner. Econ.* 35, 539–562.
40. Nassar, N.T., Graedel, T.E., and Harper, E.M. (2015). By-product metals are technologically essential but have problematic supply. *Sci. Adv.* 1, e1400180.
41. Lokanc, M., Eggert, R., and Redlinger, M. (2015). The availability of indium: the present, medium term, and long term. <https://doi.org/10.2172/1327212>.
42. Butterman, W.C., Brooks, W.E., and Reese, R.G. (2004). USGS Mineral Commodity Profiles: Cesium (USGS). <https://doi.org/10.3133/ofr20041432>.
43. Okrusch, M., and Matthes, S. (2014). *Mineralogie: eine Einführung in die Spezielle Mineralogie, Petrologie und Lagerstättenkunde* 9. Aufl (Springer Spektrum).
44. Wu, P., Wen, J., Wang, Y., Liu, Z., Lin, R., Li, H., Luo, H., and Tan, H. (2022). Efficient and thermally stable all-perovskite tandem solar cells using all-FA narrow-bandgap perovskite and metal-oxide-based tunnel junction. *Adv. Energy Mater.* 12, 2202948.
45. Klein, M., Güthner, T., Sans, J., Thalhammer, F., and Waldvogel, S.R. (2021). Sustainable and cost-efficient electro-synthesis of formamidinium acetate from cyanamide in aqueous acidic electrolyte. *Green Chem.* 23, 3289–3294.
46. Wu, G., Liang, R., Ge, M., Sun, G., Zhang, Y., and Xing, G. (2022). Surface passivation using 2D perovskites toward efficient and stable perovskite solar cells. *Adv. Mater.* 34, e2105635.
47. Jeong, J., Kim, M., Seo, J., Lu, H., Ahlawat, P., Mishra, A., Yang, Y., Hope, M.A., Eickemeyer, F.T., Kim, M., et al. (2021). Pseudo-halide anion engineering for  $\alpha$ -FAPbI<sub>3</sub> perovskite solar cells. *Nature* 592, 381–385.
48. Mattiello, S., Lucarelli, G., Calascibetta, A., Polastri, L., Ghiglietti, E., Podapangi, S.K., Brown, T.M., Sassi, M., and Beverina, L. (2022). Sustainable, efficient, and scalable preparation of pure and performing spiro-OMeTAD for perovskite solar cells. *ACS Sustainable Chem. Eng.* 10, 4750–4757.
49. Tepliakova, M.M., Akkuratov, A.V., Tsarev, S.A., and Troshin, P.A. (2020). Suzuki polycondensation for the synthesis of polytrialylamines: A method to improve hole-transport material performance in perovskite solar cells. *Tetrahedron Lett.* 61, 152317.
50. Chen, C., Zhang, S., Wu, S., Zhang, W., Zhu, H., Xiong, Z., Zhang, Y., and Chen, W. (2017). Effect of BCP buffer layer on eliminating charge accumulation for high performance of inverted perovskite solar cells. *RSC Adv.* 7, 35819–35826.
51. Strobel, R., and Pratsinis, S.E. (2007). Flame aerosol synthesis of smart nanostructured materials. *J. Mater. Chem.* 17, 4743.
52. Piccinno, F., Gottschalk, F., Seeger, S., and Nowack, B. (2012). Industrial production quantities and uses of ten engineered nanomaterials in Europe and the world. *J. Nanopart. Res.* 14, 1109.

53. Cao, X., Zhi, L., Jia, Y., Li, Y., Zhao, K., Cui, X., Ci, L., Zhuang, D., and Wei, J. (2019). A review of the role of solvents in formation of high-quality solution-processed perovskite films. *ACS Appl. Mater. Interfaces* *11*, 7639–7654.
54. Wu, C., Wang, K., Li, J., Liang, Z., Li, J., Li, W., Zhao, L., Chi, B., and Wang, S. (2021). Volatile solution: the way toward scalable fabrication of perovskite solar cells? *Matter* *4*, 775–793.
55. Roose, B., Tennyson, E.M., Meheretu, G., Kassaw, A., Tilahun, S.A., Allen, L., and Stranks, S.D. (2022). Local manufacturing of perovskite solar cells, a game-changer for low- and lower-middle income countries? *Energy Environ. Sci.* *15*, 3571–3582.
56. Heath, G.A., Silverman, T.J., Kempe, M., Deceglie, M., Ravikumar, D., Remo, T., Cui, H., Sinha, P., Libby, C., Shaw, S., et al. (2020). Research and development priorities for silicon photovoltaic module recycling to support a circular economy. *Nat. Energy* *5*, 502–510.
57. Kadro, J.M., Pellet, N., Giordano, F., Ulianov, A., Müntener, O., Maier, J., Grätzel, M., and Hagfeldt, A. (2016). Proof-of-concept for facile perovskite solar cell recycling. *Energy Environ. Sci.* *9*, 3172–3179.
58. Bogachuk, D., van der Windt, P., Wagner, L., Martineau, D., Narbey, S., Verma, A., Lim, J., Zouhair, S., Kohlstädt, M., Hinsch, A., et al. (2024). Remanufacturing perovskite solar cells and modules – a holistic case study. *ACS Sustainable Resour. Manage.* <https://doi.org/10.1021/acssusresmg.3c00042>.
59. Corsini, F., and Griffini, G. (2020). Recent progress in encapsulation strategies to enhance the stability of organometal halide perovskite solar cells. *J. Phys. Energy* *2*, 031002.
60. Ma, S., Yuan, G., Zhang, Y., Yang, N., Li, Y., and Chen, Q. (2022). Development of encapsulation strategies towards the commercialization of perovskite solar cells. *Energy Environ. Sci.* *15*, 13–55.
61. Vidal, R., Alberola-Borràs, J.-A., Habisreutinger, S.N., Gimeno-Molina, J.-L., Moore, D.T., Schloemer, T.H., Mora-Seró, I., Berry, J.J., and Luther, J.M. (2021). Assessing health and environmental impacts of solvents for producing perovskite solar cells. *Nat. Sustain.* *4*, 277–285.
62. Zhang, Y., Kim, M., Wang, L., Verlinden, P., and Hallam, B. (2021). Design considerations for multi-terawatt scale manufacturing of existing and future photovoltaic technologies: challenges and opportunities related to silver, indium and bismuth consumption. *Energy Environ. Sci.* *14*, 5587–5610.
63. Kim, S., Trinh, T.T., Park, J., Pham, D.P., Lee, S., Do, H.B., Dang, N.N., Dao, V.A., Kim, J., and Yi, J. (2021). Over 30% efficiency bifacial 4-terminal perovskite-heterojunction silicon tandem solar cells with spectral albedo. *Sci. Rep.* *11*, 15524.
64. Leijtens, T., Bush, K.A., Prasanna, R., and McGehee, M.D. (2018). Opportunities and challenges for tandem solar cells using metal halide perovskite semiconductors. *Nat. Energy* *3*, 828–838.
65. Hörantner, M.T., Leijtens, T., Ziffer, M.E., Eperon, G.E., Christoforo, M.G., McGehee, M.D., and Snaith, H.J. (2017). The potential of multijunction perovskite solar cells. *ACS Energy Lett.* *2*, 2506–2513.
66. Wang, J., Zardetto, V., Datta, K., Zhang, D., Wienk, M.M., and Janssen, R.A.J. (2020). 16.8% Monolithic all-perovskite triple-junction solar cells via a universal two-step solution process. *Nat. Commun.* *11*, 5254.
67. McMeekin, D.P., Mahesh, S., Noel, N.K., Klug, M.T., Lim, J., Warby, J.H., Ball, J.M., Herz, L.M., Johnston, M.B., and Snaith, H.J. (2019). Solution-processed all-perovskite multijunction solar cells. *Joule* *3*, 387–401.
68. Jeong, M., Choi, I.W., Go, E.M., Cho, Y., Kim, M., Lee, B., Jeong, S., Jo, Y., Choi, H.W., Lee, J., et al. (2020). Stable perovskite solar cells with efficiency exceeding 24.8% and 0.3-V voltage loss. *Science* *369*, 1615–1620.
69. Yang, D., Zhang, X., Wang, K., Wu, C., Yang, R., Hou, Y., Jiang, Y., Liu, S., and Priya, S. (2019). Stable efficiency exceeding 20.6% for inverted perovskite solar cells through polymer-optimized PCBM electron-transport layers. *Nano Lett.* *19*, 3313–3320.